Century-Scale Relative Sea-Level Changes in West Greenland – A Plausibility Study to Assess Contributions from the Cryosphere and the Ocean

Wake, L.M [1*], Milne, G. A[2], Long, A. J.[3], Woodroffe, S. A.[3], Simpson, M. J. R.[4], Huybrechts, P.[5]

[1] Department of Geography, University of Calgary, 2500 University Drive NW, Calgary, AB T2N 1N4, Canada

[2] Department of Earth Sciences, University of Ottawa, Marion Hall, Ottawa, ON K1N 6N5, Canada

[3] Department of Geography, Durham University, Science Site, South Road, Durham DH1 3LE, UK

[4] Norwegian Mapping Authority, 3507 Hønefoss, Norway

[5.] Department of Geography, Vrije Universiteit Brussel, Pleinlaan 2, B1050-Brussel, Belgium

* Corresponding author

lwake@ucalgary.ca

Phone: 1-403-210-8449

Fax: 1-403-282-6561

Abstract

This paper interprets high resolution relative sea-level (RSL) reconstructions obtained from recently deposited salt-marsh sediments in Greenland. The primary aim of this study is to determine the relative contribution to the RSL observations from local to regional ice mass changes as well as density-related (steric) variations in the adjacent ocean. At sites in west

Greenland, RSL rise slows from ~ 3mm/yr to ~ 0mm/yr at 400 years BP and is stable thereafter. In south Greenland, a similar RSL slowdown is also observed but this occurs approximately 200 years later. Substantial contributions from oceanographic changes are ruled out as dominant drivers of the RSL slowdown in western Greenland but could be more important at Nanortalik. Model sensitivity tests indicate that the RSL data are not compatible with a dominant dynamic ice loss via the Jakobshavn Isbrae outlet glacier as the region of ice loss and the resulting sea-level trends are too localised. Regional changes in ice thickness related to surface mass balance changes can explain the observed RSL signals but only if there is dominant mass loss during the period 400 years BP to present. This conclusion is unaffected even when uncertainties in Earth viscosity structure are taken into account. However, it is plausible that some of the RSL fall may be due to reduced ice growth at the onset of the Little Ice Age. A high resolution mass balance history of the Greenland Ice Sheet over the past few millennia and the influence of lateral Earth structure on predictions of RSL change are identified as priority areas of study in order to confidently separate local, 'transient' (e.g. elastic and gravitational) RSL changes from the long-term viscous contribution associated primarily with deglacial changes

Keywords: Greenland Ice Sheet, Little Ice Age, Medieval Climatic Anomaly, sea-level change, steric sea level.

1.0 Introduction

Improving current understanding of the mechanisms through which ice sheets respond to climate change is a major aim of contemporary research. The motivation for this derives, largely, from the need to improve the accuracy to which future changes in land ice and sea level can be predicted (Meehl et al., 2007). Observations of changes in ice sheets and climate, both at present

and in the past, play a central role in achieving this aim. Geodetic observations (e.g. satellite gravity and interferometry, satellite and airborne altimetry) have provided unprecedented levels of information on changes in the large ice sheets over the past few years to decades. Observations from the geological record (e.g. erosional/depositional features, sea-level changes) provide information used to constrain and test ice sheet models over millennial and longer timescales. However, there is a distinct lack of information on changes over century timescales. The work presented here and in the companion data paper (Long et al. 2011, this issue) takes some steps towards improving this situation for the Greenland Ice Sheet (GrIS).

Recent geodetic studies show that Greenland has reacted to the warming of the last decade by losing mass at its margins and thickening in some central areas, along with increased discharge from outlet glaciers. Thickening of several centimetres was recorded above 1500-2000m during 1992-2002 (Zwally et al. 2005) and over the southern part of the GrIS over the period 1997-2003 (Krabill et al. 2004). Below elevations of 1500-2000m, the ice sheet thinned on average by ~ 0.15m per year, with the thinning rate exceeding 0.25m per year in south-east Greenland around the Helheim and Kangerdlugssuaq glaciers and in parts of western Greenland (Krabill et al. 2004). The broad pattern and magnitude of these changes is also reflected in a later ATM study spanning the period of 1998-2004 (Thomas et al. 2006).The geometry of these mass changes is typical of an ice sheet reacting to a warming climate – warmer temperatures at lower elevations lead to increased thinning compared to other areas on the ice sheet and can force a positive feedback cycle of decay. Also, warmer temperatures increase moisture supply to the ice sheet, allowing the central regions to thicken (e.g. see Thomas et al. 2000, Krabill et al. 2004). Another source of mass loss from the GrIS comes from speed up of outlet glaciers. Studies (e.g. Rignot and Kanagaratnam 2006) based on satellite interferometry observed glacier acceleration in most areas since 1996. A number of processes have been proposed to explain the observed acceleration (Rignot and Kanagaratnam, 2006) and most of these are triggered by changes in air

and/or ocean temperature (e.g. Holland et al. 2008, Zwally et al. 2002). Changes in mass balance cause spatially variable RSL changes in the near and far field of an ice sheet. Patterns of mass balance may therefore be determined from relative sea-level (RSL) data such as tide gauge records and geological proxies in both near and far-field locations (e.g. see Milne et al. 2009). Over millennial timescales, reconstructions of RSL (e.g. Bennike et al. 2002; Long et al. 2003; Long et al. 2009; Sparrenbom et al. 2006a, b) and ice margin position (e.g. Bennike and Björck 2002; Funder 1989; Kelly 1980, 1985; van Tatenhove et al. 1995) provide the best constraints on changes of the GrIS, and have been used to develop models of GrIS evolution from the Last Glacial Maximum to present (e.g. Tarasov and Peltier 2002; Fleming and Lambeck 2004; Simpson et al. 2009). One common source of geological information used to reconstruct the local sea level over these time periods in Greenland is isolation basins: natural rock depressions that are tidal when below sea level but become freshwater lakes when uplifted above sea level by glacio-isostatic rebound and/or sea-level fall (see, for example, Long et al. 1999; 2009).

Millennial RSL records reconstructed from isolation basins in Greenland are typically J-shaped, recording RSL fall following ice margin retreat during the early Holocene followed by RSL rise in the late Holocene. The cause of the latter is believed to be the combined effect of the on-going collapse of the peripheral forebulges of the North American and Eurasian Ice Sheets (Fleming and Lambeck 2004) as well as renewed crustal loading in Greenland due to an expansion of the ice sheet in the so-called “Neoglacial” (Kelly 1985, Wahr et al. 2001a, b). However estimates of the relative contribution from each process vary from study to study. Between the localities considered in this paper (see Fig. 1), there are significant differences in the timing, magnitude and sign of RSL change during the late Holocene. At Aasiaat and Sisimiut, RSL rose by about 3-4m during the Neoglacial (Long et al., 2003; Long et al., 2009), whereas at Nanortalik, south Greenland, RSL rose by 6-10 m since ~5,000yrs BP (Before Present) onwards (Sparrenbom et al. 2006 a, b).

This is the first study to interpret century to decadal scale observations of RSL obtained from a near-field setting (south west Greenland). New salt marsh data (Long et al. 2011, this issue) provide constraints on local sea level over the past ~800 years that bridge the temporal data gap between millennial-scale RSL observations and those from instrumented in-situ and satellite measurements. There have been significant climate changes immediately preceding and during the period spanned by the salt marsh reconstructions. Ice core records show that from 2000 years BP, central Greenland air temperatures increased to reach a maximum around 1200-1000 years BP during which time regional air temperatures were higher than those at present. This warm interval is known at the Medieval Climatic Anomaly (MCA) (Dahl-Jensen et al. 1998). Subsequently, temperatures fell resulting in a relatively cold period between ~800-150 years BP known as the Little Ice Age (LIA). There is little direct field evidence constraining the response of the GrIS to either the MCA or the LIA.

The primary aim of this study is to determine if the salt marsh RSL reconstructions (Section 2.0) can be used to constrain changes in the GrIS that can be attributed to MCA and/or LIA conditions. The results, specifically the rates and amplitudes of ice thickness change, provide a useful context from which to interpret the more recent changes observed via geodetic techniques. Furthermore, if the ice sheet did respond significantly to these relatively recent climate changes then there will be a component signal in the present-day GIA that could impact the interpretation of geodetic data (e.g. GPS and satellite gravity). We begin by reviewing the RSL data (Section 2) and then proceed to interpret the observations in terms of regional ice changes driven by surface mass balance (3.1) and local changes associated with outlet glacier flow (3.2). In Section 3.3 we also consider the possible influences of changes in ocean density. A brief discussion and summary are given in Section 4.

2.0 Century-Scale RSL data

The sea-level history of Sisimiut, Aasiaat and Nanortalik over the past 2000 years is shown in Fig. 2. Linear regression analysis of the millennial-scale isolation basin RSL data alone (covering the last ~2000 years), using the constraint that present-day RSL is zero at each site, yields rates of 2.3 ± 0.98mm/yr (2 sigma uncertainty) at Sisimiut and 2.3mm/yr at Aasiaat (the latter rate deduced from one isolation basin data point only). The rate at Nanortalik is slightly lower, at 1.9 ± 1.1mm/yr. We note that the number of isolation basin data points used is low at all sites and that the age and height uncertainties in these data, compared to the salt marsh data, are relatively high (typically ± 200-400 years and ± 0.5 m or more (Long et al. 2009)). Not considering the century-scale sea-level records, and assuming a linear trend through recent sea-level index points to 0m at present these rates define a background millennial-scale viscous RSL trend dominated by GIA from non-Greenland sources and Neoglacial changes in the GrIS (Wahr et al., 2001a, 2001b). This technique is commonly adopted to estimate the contribution of GIA to present day sea-level change in these regions. Any departures from this trend evident in the salt marsh data are most likely due to the influence of processes in the GrIS or adjacent ocean during the past millennia.

The new salt marsh data detailed by Long et al. 2011 (this issue), used in conjunction with the isolation basin data, reveal that RSL rose at Sisimiut and Aasiaat by, 3.3 ± 0.61 mm/yr and 3.4 ± 0.72 mm/yr respectively until 400 years BP and then the rate of rise slowed to approximately 0 within data uncertainty (Fig. 2). The RSL slow-down observed in the West Greenland sites requires a reduction in the RSL trend of ~3mm/yr around 400 years BP that continues through to the present**.** The RSL history at Nanortalik over the past several hundred years is more complicated. The salt marsh data alone indicate that RSL rose rapidly from 1.5m below present at 600 years BP to ~0.25 to 0.5m below present at ~250 years BP, indicating a rise of 3.2mm/yr. Linear regression of the salt marsh data points alone indicates that the RSL trend during this time period was 4.2 ± 1.8 mm/yr. Extrapolating from ~250 years BP until present produces an RSL

rise of 1.1mm/yr indicating a slowdown similar in magnitude to that experienced at Sisimiut and Aasiaat, but occurring approximately 200 years later.

The next section of the paper explores possible causes of the RSL trends described above. In particular, we focus on interpreting the reduction in the rate of rise by ~3 mm/yr around 400 years BP at Aasiaat and Sisimiut. Specifically, we consider two regional ice evolution scenarios: one in which thinning occurs contemporaneously with the reduction in local RSL rate and one in which ice thinning occurs during the MCA (Section 3.1). The latter scenario is considered to test whether the RSL rate reduction could be associated with an ongoing viscous Earth response to a hypothesised ice loss during the MCA. Due to the proximity of the Aasiaat data site to Jakobshavn Isbrae (Fig. 1), we also calculate the (more local) ice loss required near its grounding line to force RSL rise to slow by 3mm/yr (Section 3.2). Finally, in Section 3.3, temperature and salinity data from the World Oceanographic Database 2005 (WOD05, Boyer et al. 2005) are used to generate an average profile of oceanographic conditions offshore of our data sites. These profiles are perturbed by temperature and salinity anomalies to reflect the probable conditions of the LIA and the resulting trends in steric height are calculated.

3.0 Data Interpretation

3.1 Regional ice sheet changes

Due to the lack of detailed, gridded climate data spanning the MCA-LIA, it is not possible to accurately compute regional changes in ice sheet mass balance using a glaciological model. Consequently, this section presents only a crude sensitivity analysis to gauge the magnitude and extent of ice loss in west Greenland that is required to produce a RSL fall of ~3mm/yr over the last 400 years. We focus on obtaining a fit to the data at Aasiaat and Sisimiut, and briefly comment on how the optimum solutions affect the RSL trend at Nanortalik. We test three factors that can force differences in the magnitude and spatial pattern of the near-field RSL response: the magnitude of thinning, the size of the thinning area and the timing of ice loss.

Areas of mass loss are prescribed by defining a maximum altitude of increased thinning (MAIT). Four of these are chosen based on the present-day surface elevation (Fig. 1): 500m, 1000m, 1500m, 2000m (Fig.1). Below these MAITs, four thinning rates are considered: 0.125m/yr, 0.375m/yr, 0.5m/yr and 0.625m/yr. We chose this straightforward elevation-based thinning geometry for its ease of implementation and the well-known fact that the periphery of the ice sheet is more sensitive to elevated temperatures compared to the interior. The range of thinning rates adopted was chosen on the basis of observations and modelling of ice thickness and elevation changes occurring on the GrIS. Work by Krabill et al. (2004), which analysed laser altimetry surveys and ATM flight data for 1997 to 2003, shows that the margins of the GrIS, near Jakobshavn in particular, were thinning at a rate exceeding 0.6m/yr. Over this time period, thinning was recorded at most areas in the west below the 2000m contour. In the east, elevation losses in the range 0.1 to 0.4m/yr were recorded at elevations well above 2000m. More recently, over the period 2003-2007, elevation loss in the range of 0.2-1.5m/yr was recorded along the eastern margin below the 2000m surface elevation contour, with the largest rates of loss near the Helheim and Kangerdlugssuaq outlet glaciers (Pritchard et al. 2009). Surface mass balance modelling (Wake et al. 2009), predicts that during two recent warm periods (1923-1933 and 1995-2005), the western section of the GrIS below the present-day 1500m contour thinned at rates between 0.4-5m/yr. Based on these modelling and observational results, we chose a maximum thinning rate of 0.625m/yr.

In areas where the ice surface lies above a chosen MAIT, two different rates of ice surface height change were adopted that are based on the results of a recent ice core analysis (Vinther et al. 2009). The results from this study suggest that as a whole there has been very little change in ice sheet elevation above the present 2000m contour for the past 1000 years. However, we note that a net thinning of 70m during this period is within data uncertainty. In addition, some areas (e.g. Camp Century) may have undergone thickening (maximum rate 0.12m/yr) over this

198 period. Therefore, we performed sensitivity tests that considered both a thinning of 0.07m/yr and
199 a thickening of 0.12m/yr for the region of the ice sheet above the specified MAIT. At the margin,
200 moraines from some areas in western Greenland suggest that there have been only minor
201 changes in margin position for several hundred years, with the majority of retreat (1-2km)
202 occurring only over the past 200 years (e.g. in west Greenland, Weidick 1972; Forman et al.
203 2007; Kelly and Lowell 2009). This supports our assumption that the margin positions were fixed
204 (at their current locations) during the period considered.

205 The episodes of mass loss are timed to occur at specific periods during the last 2000
206 years: 1200-800 years BP and 400 years BP. The former is compatible with an expected mass
207 loss caused by warmer conditions during the MCA, the latter to consider the case in which the
208 slowdown is due to contemporary melting of the ice. On inspection of Figure 1, it is apparent that
209 the more northerly sites (Sisimiut and Aasiaat) are close to a section of the ice sheet which at
210 present has a relatively low surface gradient and thus a relatively large area of melt extent will be
211 predicted. The present day ice margin near Nanortalik is much steeper. Even within the large
212 elevation range chosen, a very limited area in east Greenland is located below the prescribed
213 MAITs. This indicates that RSL at Sisimiut and Aasiaat will be more sensitive to the prescribed
214 ice model changes introduced above.

215 The version of the sea-level equation presented in Mitrovica and Milne (2003) and solved
216 by Kendall et al. (2005), computed to spherical harmonic degree 512, is used throughout this
217 study to calculate the RSL response at Sisimiut, Aasiaat and Nanortalik associated with ice mass
218 variations from the scenarios described above. The response of the solid Earth to changes in ice
219 load is calculated using a spherically symmetric, compressible viscoelastic Maxwell Earth model.
220 In this study the elastic and density components of Earth structure are taken from the Preliminary
221 Reference Earth Model (PREM; Dziewonski and Anderson, 1981). The viscosity structure is
222 parameterised into three layers: an upper layer with very high viscosity to simulate the lithosphere,

223 an upper mantle region that extends from the base of the lithosphere to the 670 km seismic
224 discontinuity and a lower mantle region that extends from this depth to the core–mantle boundary.
225 Due to the small amount of sub-century RSL data collected at present, we do not intend at present
226 to use these data to constrain Earth structure. We use a single Earth model with lithospheric
227 thickness (L) of 120km, upper mantle viscosity (ν_{UM}) of 0.5 x 10^{21} Pa s and lower mantle viscosity
228 (ν_{LM}) of 1 x 10^{21} Pa s. These earth model parameters were previously found to give a good fit to
229 a regional, millennial-scale RSL data set from Greenland (Simpson et al., 2009).

230 To produce the RSL curves featured in Fig. 4, the RSL change predicted using the ice
231 loading scenarios described above was added to the background trend estimated from the RSL
232 data (Fig. 2 and Section 2) in the absence of the observed slowdown. At Sisimiut and Aasiaat,
233 the background trend is 3.3 and 3.4mm/yr, respectively, up until 400 years BP. Projecting this
234 rate of RSL rise to present-day, these rates suggest sea level would be approximately 1.5m higher
235 at these sites. Therefore, our loading scenarios must produce a total of ~1.5m sea level fall over
236 the last 400 years to counteract the ongoing RSL rise associated with viscous deformation thought
237 to be dominated by Neoglacial regrowth of the GrIS and deglaciation of the North American (and
238 to a lesser extent, Eurasian) Ice Sheets. That is, we seek to produce a RSL curve that is
239 approximately level over the last 400 years, consistent with the data points in Fig. 2.

240 Inspection of the chi-squared plots in Fig. 3 indicates that irrespective of the timing of
241 peripheral melt (400-0 years BP, Panel A; 1200-800 years BP, Panel B), loading histories with a
242 central region of growth at a rate of 0.12m/yr (plots labelled ‘G’) require thinning of in excess of
243 0.375m/yr in all regions below the 2000m contour in order to produce a reasonable fit to the RSL
244 data (Fig. 4). These thinning rates would have resulted in a net ice surface lowering of at least
245 150m below the 2000m contour during a 400 year period. Given that this central ice sheet growth
246 rate is an end member scenario from Vinther et al. (2009), and only representative of the area
247 near Camp Century, we conclude that the thinning rates required for this set of experimental

parameters are unlikely. Consequently, the remaining discussion in this section focuses on the scenarios in which this region of the ice sheet above the specified MAIT thins at the rate of 0.07m/yr (Fig. 3, Panels A and B, plots labelled 'L').

When the central areas of the ice sheet are losing mass the amount of ice loss required at lower elevations is reduced when thinning is restricted to the period from 400 years BP to present. If thinning is restricted to the area below the 1500m contour the best fit to the data can be achieved by thinning of 0.375m/yr, the net ice loss from 400 years BP being 150m (see Table 1). However, by increasing the area exposed to a higher thinning rate (i.e. to include the entire area below the 2000m contour), the RSL data can be matched equally well with rates of thinning as low as approximately 0.15m/yr. This results in a total net surface lowering of ~60m below the 2000m contour since 400 years BP.

When comparing the *timing* of ice loss (compare plots labelled 'L' in Fig. 3), statistically equivalent fits to the data can be achieved when peripheral melt is initiated in either the LIA or MCA. In the case of MCA mass loss, best fit models reside in the parameter space where the high thinning rates (>0.5m/yr) are concentrated generally up to the 2000m contour (Fig 3, Panel B, Table 1). Allowing a thinning rate of 0.07m/yr in the centre of the ice sheet does not reduce the minimum required ice loss compared to the growth scenario, nor the area over which it is required to occur (Fig. 3, Panel B, compare plots L and G). Visual inspection of the RSL curves produced by the best fit models for MCA mass loss (Fig. 4, Panel B) shows that even though a significant degree of model-data fit is achieved, the model RSL curve diverges significantly from the older sea-level index points located at 1200-1400 years ago at Aasiaat and Sisimiut. Moreover, a RSL highstand such as that predicted at c. 800 years BP would have left a distinct stratigraphic signature in the salt marshes which is not observed (Long et al., 2010; 2011 this issue), and therefore this scenario (Figs. 3 and 4, Panel B) is not supported.

The RSL curves produced by the best fit models of our preferred timing of mass loss (Fig. 4 Panel A, Table 1) demonstrate that there is spatial sensitivity of the RSL response to ice loading. Although the pre-LIA RSL rise at Sisimiut and Aasiaat calculated from the RSL data is similar in magnitude, the RSL response to ice loading is larger at Aasiaat compared to Sisimiut. In Panel A, some best fit models predict sea level rising 0.2-0.5m above present at Aasiaat. High marsh sediments (Long et al. 2011, this issue) indicate a possible maximum RSL highstand of only 0.2m at Aasiaat. In all cases, the RSL response at Nanortalik is smaller compared to that in Aasiaat and Sisimiut. Although it is closer to the ice margin, the predicted RSL fall is lower because the steep margin does not allow for a large extent of the ice sheet to be exposed to thinning. It is also clear that initiating mass loss at 400 years BP, which is suitable for Sisimiut and Aasiaat, deflects the background RSL trend at Nanortalik. However, when considering the RSL response at Nanortalik as a result of the best fit models in Table 1, the predicted sea-level change occurring 400 years BP and continuing until present lies in the range of -1.7 to -1mm/yr. As stated earlier, the uncertainty in the trend at Nanortalik from 600-200 years BP is ± 1.8mm/yr. Therefore, it is possible that a RSL slowdown did occur at Nanortalik at 400 years BP, since the magnitude of change is below the detection threshold of the observations.

Additional calculations (not shown) indicate that over the range of Earth parameters considered to provide a reasonable fit to millennial-scale data in the study by Simpson et al. (2009) (L=96-120km, $v_{UM} > 0.4 \times 10^{21}$ Pa s and 1×10^{21} Pa s $< v_{LM} < 50 \times 10^{21}$ Pa s) , the sea-level trends at Aasiaat and Sisimiut vary by at most a few tenths of a mm/yr with the variation at Aasiaat being larger that at Sisimiut due to its increased proximity to the ice margin. This sensitivity to Earth model uncertainty is not large enough to significantly influence the chi-squared results (Fig. 3) such that it would affect the conclusions of our analysis.

Even though we have tested a limited range of scenarios, it is important to assess these mass balance changes of the GrIS in terms of their potential eustatic contributions to sea level

297 change over the past 400 years. The associated contribution to eustatic sea-level change for our
298 preferred suite of models (i.e. those where the melt is focussed after 400 years BP, Table 1) lies
299 in the range of 0.27-0.5mm/yr. However, we stress that this is an upper bound on Greenland's
300 contribution since the RSL data are mainly sensitive to ice thickness changes in the south-west
301 sector of the ice sheet. Far-field RSL records indicate that the average rate of global mean sea-
302 level rise has been no more than a few tenths of a mm/yr for the past 2000 years (Milne et al.
303 2009). But, the contribution of other factors such as mountain glacier and Antarctic Ice Sheet
304 mass balance over the last 2000 years is largely unknown and may well be negative.

305 Finally, the work carried out in this paper assumes that the 'background' RSL trend
306 (Section 2) is wholly viscous in origin, and derives from collapse of the forebulge of the North
307 American ice sheets and Neoglacial regrowth of the western margin of the GrIS. The loading
308 models for the MCA and LIA are considered only for their ability to produce short-term departures
309 from the secular background trend, specifically with regard to predicting stable sea levels during
310 the past 400 years at Aasiaat and Sisimiut. Because of this assumption, the maximum required
311 RSL fall due to negative LIA mass balance is 3mm/yr. In reality, some of the RSL deceleration
312 400 years BP could be due to the cessation of a RSL rise sourced from ice sheet growth during
313 the MCA (a period of a predominantly positive North Atlantic Oscillation, Trouet et al. 2009). To
314 address these issues a more complete analysis that considers GrIS changes over the past few
315 millennia using climate-forced glaciological models is necessary.

316 **3.2 Localised thinning at Jakobshavn Ice Stream**

317 Since two of the salt marsh data sites (Sisimiut, and in particular Aasiaat) are proximal to
318 Jakobshavn Isbrae, it is important to assess how ice thickness changes here can affect local sea
319 level, and how far these effects extend spatially. To address this, we constructed a simple
320 experiment that is based on the recent work of Khan et al. (2010), in particular Fig. 5a from this

publication, to delineate an approximate area of focussed thinning associated with drawdown of ice from Jakobshavn Isbrae. The sea-level response is calculated as in Section 3.1. During 2006-2009, the area within the region of 68.75-69.5^{o}N and 48-50^{o}W underwent and average thinning of approximately 4-10m/yr. This rate increased with proximity to the grounding line; increasing from 12m/yr at a distance of 20km up to 28m/yr within 5km. Khan et al. (2010) predict that with this loading configuration, the elastic uplift rate at Aasiaat would be 1.4mm/yr, compared to 12.1mm/yr at the grounding line. Due to the ice loss being focussed in a small (~ 80km x 80km) area, the resulting pattern of sea-level change is extremely localised.

In Fig. 5, the ice loss is fixed to 4m/yr. For this mass loss configuration and this Earth model, the required sea-level fall of 3mm/yr is predicted at Aasiaat. If sustained over century timescales this degree of thinning would be able to fully account for the RSL fall at Aasiaat but less than 30% of that at Sisimiut. A 3mm/yr RSL fall at Sisimiut can be generated by scaling the ice loss by approximately a factor of 4. However, this causes a 12mm/yr fall at Aasiaat, which is clearly not supported by the RSL data. The above results show that, while ice thickness changes associated with discharge from JI can account for a portion of the observed sea-level slowdown, the spatial gradient associated with the predicted RSL signal rules it out as a dominant contributor. Furthermore, as indicated above, a discharge rate of tens of km^3/yr is likely to be restricted to years of warmer temperatures and is not reflective of LIA conditions. Indeed, Jakobshavn Isbrae attained its maximum late Holocene extent at some time during the Little Ice Age (Weidick and Bennike 2007, Briner et al. 2010). Further examination of the contribution of Jakobshavn Isbrae to local RSL change would benefit from additional RSL data from close to the outlet glacier where the predicted RSL gradients are steepest.

3.3 Steric influences on Greenland relative sea level

We now explore the potential contribution of steric processes to RSL change in Greenland using temperature and salinity profiles downloaded from the online 2005 World Oceanographic Database (WOD05, Boyer et al., 2005). For the calculation of steric height trends only Ocean Station Data are used since this instrument type has the longest continuous record of data in this area. We use raw oceanographic profiles from the WOD05 in preference to interpolated World Oceanographic Atlas (WOA) data to reduce any bias that may have been introduced during the interpolation process (Miller and Douglas, 2004). The location and maximum depth of measurements of the temperature and salinity profiles used are detailed in Fig. S1 and Table S1 (see online supporting material). Steric height is calculated by integrating over depth the density (and therefore specific volume) changes in the water column. At all depths in the water column, the specific volume of sea water is calculated relative to the specific volume occupied by sea water of salinity 35 psu and temperature 0^{o}C at the same pressure (i.e. depth) in the water column. The calculations of steric height are based on the Equation of State of Sea Water (Fofonoff and Millard, 1983), incorporated in a computer algorithm provided by P. Woodworth (*pers. comm.).*

We calculated steric height anomalies for five specific depth ranges in Davis Strait (0-50m, 0-150m, 0-300m and 0-500m and 0-1000m) and seven depth ranges at Nanortalik (as for Davis Strait but including 0-2000m and 0-3000m). These depth levels were chosen to reflect approximate depths of transition between specific water bodies in the Disko Bugt area: Polar Water ~ 50m to 300m; West Greenland Current ~ below 300m (Lloyd, 2006) and sharp changes in the thermocline. For steric height variations calculated to a reference level of 50m from the period 1928-1990, linear regression performed on the series shows a trend in dynamic height in the Davis Strait area between latitudes of 65-71^{o}N of 0.19± 0.06mm/yr (2σ uncertainty, Table S1). The slight increase of steric height in the upper 50m suggests that warming and/or freshening has occurred over the past several decades, possibly reflecting changes in runoff from the ice sheet. Integrating over the upper 300m produces a similar result. Integration over the entire

depth interval of 1000m shows an overall positive trend of 2.1±0.7mm/yr for the Davis Strait area, but we note that there are large gaps in data between 1928-1949 and 1974-1985.

It may be appropriate for Aasiaat and Sisimiut to calculate steric trends only to a depth of 500m, since the continental shelf in west Greenland extends for ~100km from the coast at Sisimiut where the water depth remains between 200 and 400m (Fig S1). In Disko Bugt, north of Aasiaat, the water depth remains shallower than 500m, apart from a narrow trough of ~ 800m depth extending from the mouth of Jakobshavn Isbrae. Integrating density changes to 500m depth gives a steric rise of 1.4 ± 0.37mm/yr for this region. We note that, in this area, our analysis of the 20^{th} century trends in steric height is hampered by poor temporal coverage of temperature and salinity profiles since trends are largely based on data collected in spring and summer months (see Table S1) and therefore not reflective of trends in mean annual steric height.

At Nanortalik, the steric height trend is predicted to be slightly negative but does not show a large magnitude variation when summing to different depth levels. When considering the full depth range (0-3000m) and 2σ uncertainty, the trend in dynamic height is predicted to be -1.3±1.1mm/yr for the period of 1935-1997. Although this is enough to account for some of the required RSL fall, we note, again, that this result must be interpreted with caution since it was calculated using a low number of data points collected primarily in spring and summer months (Table S1). We conclude that the magnitude of the steric sea-level fall at Nanortalik for 1935-1997 is likely to be only a few tenths of a mm/yr in magnitude.

In the absence of data pertaining to oceanographic conditions during the LIA, we carry out a sensitivity analysis to determine if steric changes could have been a significant contributor to the observed changes in RSL at Sisimiut and Aasiaat at 400 years BP. To perform such an analysis, reference temperature and salinity profiles must be produced so that perturbations to these reference states can be considered. Due to the sparseness of data from Arctic waters, a

single pair of temperature and salinity profiles calculated from data contained between 65-71ºN and 65 to 50ºW is utilised and assumed to be representative of conditions at both Sisimiut and Aasiaat (Fig. S2, supporting online material). In Davis Strait, the upper 50m are the freshest part of the water column, with salinity typically less than 34 psu (Fig S2). In general, salinity increases with depth, with the variation of salinity (typically ±1.5 psu at the 2-sigma level) tending to decline with depth. However, this scatter is most likely an artefact of the decline of number of data points with depth. Upper waters are generally warm (2-4ºC) due to solar heating, but the incursion of Polar Water (Lloyd, 2006a)) at depths between 50m and 300m reduces the temperature between these levels to between 0 and 2ºC. The warm, saline deep water body below 300-500m depth in west Greenland is due to the northward movement of the West Greenland Current.

Temperature and salinity perturbations were applied linearly over time and over specific depth ranges which are given in the caption for Fig. 6. What is immediately apparent from Fig. 6 is the relatively small influence on steric height from temperature changes compared to salinity changes. In Fig. 6A, for any given salinity anomaly the change of steric height trend over the range of temperature anomalies is approximately 0.25mm/yr. In comparison for the range of salinity trends considered (0-0.005 psu/yr), the total differences in the predicted trends are 2.25mm/yr and 1.75mm/yr in Fig. 6A and B, respectively. These results indicate the importance of salinity variations in steric height calculations compared to equivalent magnitude temperature trends. To account for half of the required 3mm/yr sea-level fall since 400 years BP observed at Aasiaat and Sisimiut, the upper 500m of the surrounding ocean would require a substantial salinity increase of 0.003-0.005 psu/yr (1.2- 2 psu since 400 years BP).

In summary, whilst the variations in temperature and salinity considered can produce the desired sea-level fall (Fig. 6), such changes would likely have led to dramatic and secular shifts in the oceanographic regime that are difficult to support with current evidence. Analyses of salinity data from the North Atlantic suggest that this region is unlikely to show a net increase or decrease

418 of ~1-2psu over 400 years (0.003-0.005 psu/yr). These trends in salinity are almost an order of
419 magnitude larger than those occurring at present day in the majority of the world's oceans (Boyer
420 et al. 2005). Additionally, a modelling study by Sedlacek and Mysak (2008) demonstrated that the
421 maximum difference between the zonal mean salinity at high latitudes between 1500-1850 and
422 1850-2000 at any depth level was no larger than ±0.1psu. Other evidence to argue against a
423 major contribution from steric changes is found in a study by Levine and Bigg (2008), who
424 demonstrated that major climatic variations such as Heinrich events are required to force long-
425 term changes in salinity similar in magnitude to those explored in Fig. 6.

426 **4.0 Conclusions**

427 RSL data from salt marshes (Long et al. 2011, this issue) show that sea level rose at
428 Aasiaat and Sisimiut at a rate of ~3mm/yr from 0 A.D. until 1600 A.D. and then remained stable
429 thereafter. At Nanortalik, a slowdown in RSL of similar magnitude occurs ~ 200 years later. The
430 primary aim of this study is to make a first attempt at determining which of three processes is
431 most likely to have caused the deceleration in RSL at these locations in south west Greenland.
432 Three processes were considered: regional ice thinning related to surface mass balance change,
433 local thinning related to changes in Jakobshavn Isbrae dynamics, and sea-surface fall due to
434 changes in the temperature and salinity of the adjacent ocean.

435 We used our RSL data to test two different models of regional ice mass loss: one in which
436 mass was lost during the MCA and the other in which mass was lost subsequent to the timing of
437 the RSL deceleration. RSL predictions forced by a period of mass loss during the Medieval
438 Climate Anomaly (MCA) do not match the RSL observations for a range of adopted MAITs and
439 thinning rates. In contrast, a period of regional-scale ice loss contemporary with the reduced rates
440 of RSL rise (during the LIA) results in a good fit to observations.

441 A dominant signal due to thinning proximal to the grounding line of Jakobshavn Isbrae is
442 unlikely. Our results show that the local ice thinning associated with this process results in a large
443 spatial gradient in the RSL fingerprint and this is not evident in the observations. Changes in
444 temperature and salinity cannot be ruled out as a key contributor to RSL fall throughout most of
445 the 20th century at Nanortalik. A sensitivity analysis shows that salinity changes could potentially
446 have produced the ~3mm/yr deceleration at the other two sites but the magnitude of the changes
447 required over several centuries is extremely unlikely. Finally, the possibility of a eustatic
448 contribution from non-Greenland ice can be ruled out since this would have resulted in the same
449 signal at all three sites.

450 Within the parameter range explored in this study, our preferred scenario is regional ice
451 thinning dominated by a surface mass balance response to elevated air temperatures since 400
452 years BP. This scenario requires an increase in air temperatures in the south west sector of the
453 GrIS from 400 years BP to present. Temperature changes estimated from the GRIP and DYE-3
454 ice cores (Dahl-Jensen et al. 1998) suggest a cooling at this time, consistent with the occurrence
455 of the LIA recorded in Europe. Long et al. 2011 (this volume) propose that the inflexion in the RSL
456 trend in west Greenland occurring 400 years ago may have been driven by a change in mode of
457 the North Atlantic Oscillation, as reported in Trouet et al. (2009). Significant relationships between
458 seasonal and mean annual temperatures, accumulation and melt extent and the NAO in west
459 Greenland and elsewhere have been noted in several studies (Appenzeller et al. 1998; Hanna
460 and Cappellen 2003; Mosely-Thompson et al. 2005; Box 2006; Chen et al. 2009). A large NAO-
461 driven response (Long et al. 2011, this volume) of the south west sector of the GrIS over the past
462 400 years serves as a working hypothesis that can be tested further via both observational and
463 modelling initiatives. Finally, it is worth reiterating that the results presented in this study do not
464 represent the definitive interpretation of the RSL observations and that the primary aim was to
465 determine the mechanisms that could have been responsible for the observed RSL deceleration.

Our results indicate that, of the processes considered, contemporary peripheral thinning of the GrIS (south west sector) is the most likely dominant contributing mechanism. This plausibility study is a useful precursor to the application of more sophisticated glaciological ice models to test our ideas further.

Acknowledgements

The research was completed as part of NERC Grant NE/C519311/1. LMW acknowledges funding support from the Canadian Institute for Advanced Research (CIFAR). GAM acknowledges funding support through the Natural Sciences and Engineering Research Council of Canada and the Canada Research Chairs program. We thank Shawn Marshall for useful discussions that have contributed to the work presented in this paper.

Figure Captions

Figure 1: Map showing positions of salt marsh data sites (circles), ice cores (squares) and other locations mentioned in this text. The 500m (solid line), 1000m (dashed line), 1500m (dot-dashed line) and 2000m (dotted) elevation contours for the GrIS at present (area coloured gray) are highlighted.

Figure 2: RSL reconstructions at the three sites considered in this paper. Plots in Panel A give an overview of RSL change at the three data sites over the last two millennia. Panel B focuses on the period covered by the new proxy RSL data (last 800 years). Key: ^{14}C-dated isolation basin-derived RSL data (black triangles, Aasiaat: Long et al. (2003), Sisimiut: Long et al. (2009), Nanortalik: Sparrenbom et al. (2006a), Bennike et al. (2002)); ^{14}C-dated salt marsh-derived RSL data (white squares, Long et al., 2011, this issue).

Figure 3: Chi squared plots displaying the degree of misfit for combinations of ice thinning rates (y axis) and chosen MAIT values (x axis). The chosen period of thinning is timed to coincide with the observed slowdown in RSL at (400 yrs BP to present, Panel A) and the Medieval Climatic Anomaly (1200-800yrs BP, Panel B). The chi-squared plots labelled 'G' (growth) and 'L' (loss) refer to the adopted rate of ice thickness change above the prescribed MAIT: +0.12 and -0.07m/yr, respectively. Dotted lines in the chi-squared plots denote the combinations of thinning rate and thinning area which produce RSL trends with a statistically equivalent fit (95% confidence interval).

Figure 4: RSL curves at each site calculated using optimal model parameters (see Table 1 for key). Panel A shows results for thinning during the period from 400 years BP to present and Panel B shows results for thinning during the period 1200-800 years BP.

Figure 5: RSL fingerprint illustrating the local sea-level change generated by thinning of Jakobshavn Isbrae. The predicted sea-level change represents the immediate (elastic) land deformation and gravitational response to ice loss of 4m/yr over the region outlined, corresponding to an ice volume loss of 26 km^3/yr. The grounding line of Jakobshavn Isbrae is marked with a star. Note that the sea-level fingerprint may be linearly scaled for differing rates of ice loss or growth.

Figure 6: Predicted trends in steric height for cooling and salinification (Panel A) and warming and salinification (Panel B) of the upper 500m of the water column. These perturbations are applied to represent plausible changes to the water during a LIA climate. Panel A represents trends in steric height analogous to increased influence of the cold, saline East Greenland Current in the West Greenland Current described in Lloyd (2006b). Panel B represents increased influence of

warm saline Atlantic Water in the West Greenland Current during the LIA (e.g. as in Krawczyk et al. (2010))

Table Captions

Table 1: Details of the best fit model combinations obtained from the chi-squared analysis in Fig. 3

References

Appenzeller, C., Stocker, T. F., Anklin, M., 1998. North Atlantic Oscillation Dynamics Recorded in Greenland Ice Cores. Science 282, 446-449

Bennike, O., Björck, S., Lambeck, K., 2002. Estimates of South Greenland late-glacial ice limits from a new relative sea-level curve. Earth and Planetary Science Letters 197, 171–186.

Bennike, O., and Björck, S., 2002. Chronology of the last recession of the Greenland Ice Sheet. Journal of Quaternary Science 17 (3), 211–219

Box, J. E., 2006. Greenland ice sheet surface mass-balance variability: 1991–2003. Annals of Glaciology 42 (1), 90-94

Boyer, T. P., Antonov, J.I. , Garcia, H.E., Johnson, D. R., Locarnini, R. A., Mishonov, A.V., Pitcher, M.T., Baranova, O.K., Smolyar, I.V., 2006. World Ocean Database 2005 in Levitus, S. (Ed.), NOAA Atlas. NESDIS 60, U.S. Government Printing Office, Washington, D.C., 1- 190

Briner, J. P., Stewart, H. A. M., Young, N. E., Philipps, W., Losee, S., 2010. Using proglacial-threshold lakes to constrain fluctuations of the Jakobshavn Isbrae ice margin, western Greenland, during the Holocene. Quaternary Science Reviews 29, 3861-3874.

534 Chen, L., Johannessen, O. M., Khvorostovsky, K., Wang, H., 2009. Greenland Ice Sheet
535 Elevation Change in Winter and Influence of Atmospheric Teleconnections in the Northern
536 Hemisphere. Atmospheric and Oceanic Science Letters 2(6), 376-380

537 Dahl-Jensen, D., Mosegaard, K., Gundestrup, N., Clow, G. D., Johnsen, S. J., Hansen, A.W.,
538 Balling, N., 1998. Past temperatures directly from the Greenland Ice Sheet. Science, 282, 268-
539 271.

540 Dziewonski, A. M., Anderson D. L., 1981. Preliminary reference Earth model. Physics of the Earth
541 and Planetary Interiors 25, 297–356.

542 Fleming, K., Lambeck, K., 2004. Constraints on the Greenland ice sheet since the Last Glacial
543 Maximum from sea-level observations and glacial-rebound models. Quaternary Science Reviews
544 23 (9–10), 1053–1077.
545
546 Fofonoff, N. P., Millard, R. C., 1983. Algorithms for computation of fundamental properties of
547 seawater. UNESCO Technical Papers in Marine Science 44, 1-53

548 Forman, S. L. , Marín, L., Van Der Veen C., Tremper, C., Csatho, B. 2007. Little Ice Age and
549 Neoglacial landforms at the Inland Ice margin, Isunguata Sermia, Kangerlussuaq, west
550 Greenland. Boreas 36, 341-351.

551 Funder, S., 1989. Quaternary geology of the ice-free areas and adjacent shelves of Greenland.
552 In: Fulton, R.J. (Ed.), Quaternary Geology of Canada and Greenland. Geological Survey of
553 Canada, 741–792.

554 Hanna, E., Cappelen, J., 2003. Recent cooling in coastal southern Greenland and relation with
555 the North Atlantic Oscillation. Geophysical Research Letters 30(3) 1132.
556 doi:10.1029/2002GL01579

Holland, D. M., Thomas, R. H., De Young, B., Ribergaard, M. H., Lyberth, B. 2008. Acceleration of Jakobshavn Isbrae triggered by warm subsurface ocean waters. Nature Geoscience 1, 659-664.

Kelly, M., 1980. The status of the Neoglacial in western Greenland. Rapport Grønlands Geologiske Undersøgelse 96, 24.

Kelly, M., 1985. A review of the Quaternary Geology of western Greenland, in: Andrews, J. T. (Ed), Quaternary Environments: Eastern Canadian Arctic, Baffin Bay and Western Greenland. Allen and Unwin, Boston, pp. 461–501

Kelly, M.A., Lowell, T.V., 2009. Fluctuations of local glaciers in Greenland during latest Pleistocene and Holocene time. Quaternary Science Reviews 28, 2088-2106.

Kendall, R., Mitrovica, J. X., Milne, G. A. 2005. On post-glacial sea level – II. Numerical formulation and comparative results on spherically symmetric models. Geophysical Journal International 161, 679-706.

Khan, S.A., Liu, L., Wahr, J., Howat, I., Joughin, I., van Dam, T., Fleming, K., 2010. GPS measurements of crustal uplift near Jakobshavn Isbrae due to glacial ice mass loss. Journal of Geophysical Research-Solid Earth 115, B09405.

Krabill, W., Hanna, E., Huybrechts, P., Abdalati, W., Capellen, J., Csatho, B., Frederick, E., Manizade, S., Martin, C., Sonntag, J., Swift, R., Thomas, R., Jungel, R., 2004. Greenland Ice Sheet: Increased coastal thinning. Geophysical Research Letters 32. L24402. doi:10.1029/2004GL021533

579 Krawczyk, D., Witkowski, A., Moros, M., Lloyd, J., Kuijpers, A., Kierzek, A., 2010. Late-Holocene
580 diatom-inferred reconstruction of temperature variations of the West Greenland Current from
581 Disko Bugt, central West Greenland. The Holocene 20 (5), 659-666

582 Levine, R. C., Bigg, G. R., 2008. Sensitivity of the glacial ocean to Heinrich events from different
583 iceberg sources, as modelled by a coupled atmosphere-iceberg-ocean model. Paleoceanography
584 23, doi:10.1029/2008PA001613.

585 Lloyd, J. M., 2006a. Modern distribution of benthic foraminifera from Disko Bugt, West Greenland.
586 Journal of Foraminiferal Research, 2006. 36(4), 315-331.

587 Lloyd, J. M., 2006b. Late Holocene environmental change in Disko Bugt, west Greenland:
588 interaction between climate, ocean circulation and Jakobshavn Isbrae. Boreas 35:1, 35 — 49
589

590 Long, A. J., Roberts, D. H., Wright, M. R., 1999. Isolation basin stratigraphy and Holocene relative
591 sea-level change on Arveprinsen Ejland, Disko Bugt, West Greenland. Journal of Quaternary
592 Science 14 (4), 323-345.

593 Long, A. J., Roberts, D. H., Rasch, M., 2003. New observations on the relative sea level and
594 deglacial history of Greenland from Innaarsuit, Disko Bugt. Quaternary
595 Research 60 (2), 162–171.

596 Long, A. J., Woodroffe, S. A., Dawson, S., Roberts, D. H. Bryant, L. M. 2009. Late Holocene
597 relative sea-level rise and the Neoglacial history of the Greenland Ice Sheet. Journal of
598 Quaternary Science 24(4), 345-359

599 Long, A. J., Woodroffe, S. A., Milne, G. A., Bryant, C. L., Wake, L. M., 2010. Relative sea-level
600 change in West Greenland during the last millennium. Quaternary Science Reviews 29, 367-383.

601 Long, A. J., Woodroffe, S. A., Milne, G. A., Bryant, C. L., Simpson, M. J. R., Wake, L. M., 2011.
602 Relative sea-level change in Greenland during the last 800 years and the response of the ice
603 sheet to the Little Ice Age. Earth and Planetary Science Letters PALSEA special edition

604 Meehl, G. A. et al. 2007. Global Climate Projections. In: Solomon, S., D. Qin, M. Manning, Z.
605 Chen, M. Marquis, K.B. Averyt, M.Tignor and H.L. Miller (Eds.). Climate Change 2007: The
606 Physical Science Basis. Contribution of Working Group I to the Fourth Assessment Report of the
607 Intergovernmental Panel on Climate Change Cambridge University Press, Cambridge, United
608 Kingdom and New York, NY, USA.

609 Miller, L., Douglas, B. C., 2004 Mass and volume contributions to twentieth-century global sea-
610 level rise. Nature 428, 406-409.

611 Milne, G. A., Gehrels, W. R., Hughes, C. W., Tamisiea, M. E., 2009. Identifying the causes of sea-
612 level change. Nature Geoscience 2, 471-478

613 Mitrovica, J. X., Milne, G. A., 2003. On post-glacial sea level: I. General theory. Geophysical
614 Journal International 154, 253–267.

615 Mosley-Thompson, E., Readinger, C. R., Craigmile, P., Thompson, L. G., Calder, C. A., 2005.
616 Regional sensitivity of Greenland precipitation to NAO variability. Geophysical Research Letters
617 32, L24707. doi:10.1029/2005GL024776.

618 Pritchard, H. D., Arthern, R. J., Vaughan, D. G., Edwards, L. A., 2009. Extensive dynamic thinning
619 on the margins of the Greenland and Antarctic ice sheets. Nature 461, 971-975.

620 Rignot, E, Kanagaratnam, P 2006. Changes in the Velocity Structure of the Greenland Ice Sheet.
621 Science 311, 986-990.

622 Sedlacek, J., Mysak, L. A., 2008. A model study of the Little Ice Age and beyond: changes in
623 ocean heat content, hydrography and circulation since 1500. Climate Dynamics, 817-831.

624 Simpson, M. J. R., Milne, G. A., Huybrechts, P., Long, A. J. 2009. Calibrating a glaciological model
625 of the Greenland ice sheet from the Last Glacial Maximum to present-day using field observations
626 of relative sea level and ice extent. Quaternary Science Reviews 28 (17-18), 1631-1657.

627 Sparrenbom, C. J., Lambeck, K., Bennike, O. and Björck, S., 2006a. Holocene relative sea-level
628 changes in the Qaqortoq area, southern Greenland. Boreas 35 (2), 171-187.

629 Sparrenbom, C.J., Bennike, O., Björck, S. and Lambeck, K., 2006b. Relative sea-level changes
630 since 15 000 cal. yr BP in the Nanortalik area, Southern Greenland. Journal of Quaternary
631 Science 21 (1), 29-48.

632 Tarasov, L., Peltier, W.R., 2002. Greenland glacial history and local geodynamic consequences.
633 Geophysical Journal International 150 (1), 198–229
634
635 Thomas, R., Frederick, E., Krabill W.,Manizade, S and Martin, C., 2006, Progressive increase in
636 ice loss from Greenland, Geophysical Research Letters, 33, L10503, doi:10.1029/
637 2006GL026075
638
639 Thomas, R., Akins, T., Csatho, B., Fahnestock, M., Gogineni, P., Kim, C., Sonntag, J., 2000. Mass
640 balance of the Greenland ice sheet at high elevations. Science 289, 426–428.

641

642 Trouet, V., Esper, J., Graham, N. E., Baker, A. Scourse, J. D. Frank, D. C., 2009. Persistent
643 Postive North Atlantic Oscillation Mode Dominated the Medieval Climate Anomaly. Science 324,
644 78-80

Van Tatenhove, F.G.M., van der Meer, J.J.M., Huybrechts, P., 1995. Glacial–geological geomorphological research in west Greenland used to test an ice-sheet. Quaternary Research 44 (3), 317–327.

Vinther, B.M., Buchardt, S. L., Clausen, H. B., Dahl-Jensen, D., Johnsen, S. J., Fisher, D. A., Koerner, R. M., Raynaud, D., Lipenkov, V., Andersen, K. K., Blunier, T., Rasmussen, S. O., Steffensen, J. P., Svensson, A. M. 2009. Holocene thinning of the Greenland ice sheet. Nature 461, 385-388

Wahr, J. van Dam, T., Larson, K., Francis, O. 2001a. Geodetic measurements in Greenland and their implications. Journal of Geophysical Research 106 B8, 16567-16581.

Wahr, J. van Dam, T., Larson, K., Francis, O. 2001b. GPS measurements of vertical crustal motion in Greenland. Journal of Geophysical Research 106 D24 33755-33759.

Wake, L. M., Huybrechts, P., Box, J. E., Hanna, E. Janssens, I., Milne, G. A., 2009. Surface mass-balance changes of the Greenland ice sheet since 1866. Annals of Glaciology 50, 178-184

Weidick, A., 1972. Holocene shore-lines and glacial stages in Greenland - an attempt at correlation. Grønlands Geologiske Undersøgelse 41, 1-39.

Weidick, A. and Bennike, O., 2007. Quaternary glaciation history and glaciology of Jakobshavn Isbrae and the Disko Bugt region, West Greenland: a review. Geological Survey of Denmark and Greenland Bulletin 14, 1-13.

Zwally, H. J., Giovinetto, M. B. , Li, J., Cornejo, H. G. , Beckley M. A., Brenner, A. C., Saba, J. L., Yi, D., 2005. Mass changes of the Greenland and Antarctic ice sheets and shelves and contributions to sea-level rise 1992-2002. Journal of Glaciology 51 (175). 509-524.

Zwally, H. J., Abdalati, W., Herring, T., Larson,K., Saba, J., Steffen, K., 2002. Surface Melt-Induced Acceleration of Greenland Ice-Sheet Flow, Science 297 (5579) 218 – 222.

Figures

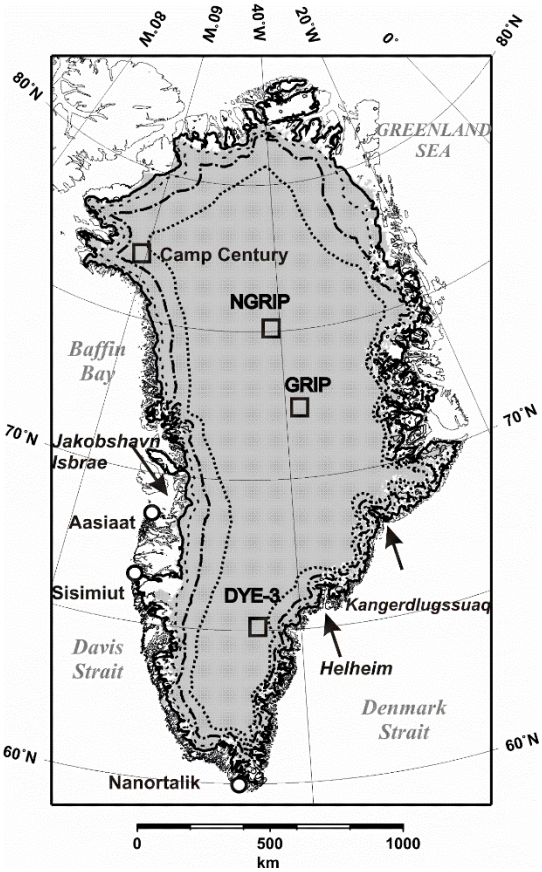

689

690 Figure 1: Map showing positions of salt marsh data sites (circles), ice cores (squares) and other
691 locations mentioned in this text. The 500m (solid line), 1000m (dashed line), 1500m (dot-dashed
692 line) and 2000m (dotted) elevation contours for the GrIS at present (area coloured gray) are
693 highlighted.

694

695

696

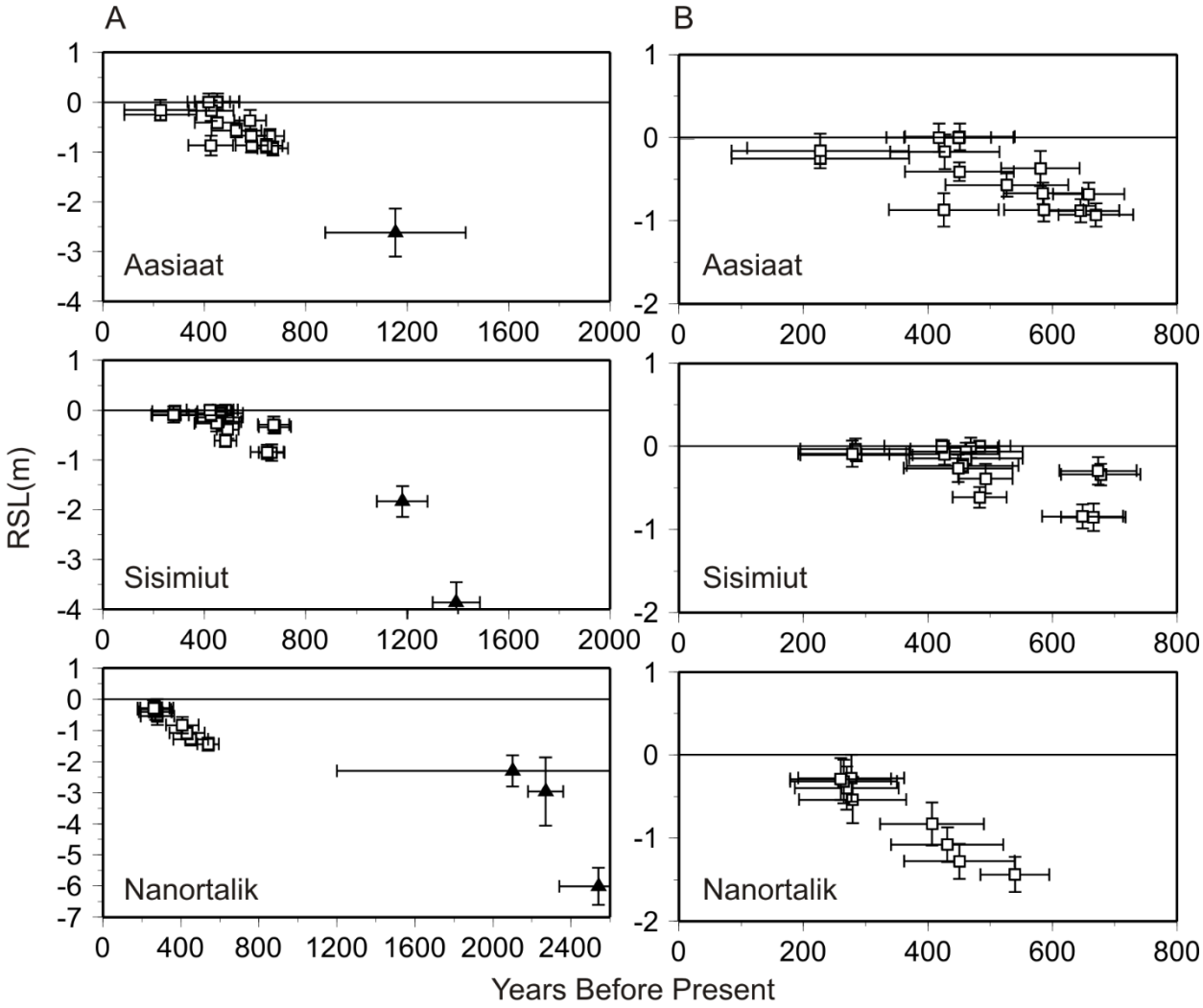

697

698 Figure 2: RSL reconstructions at the three sites considered in this paper. Plots in Panel A give an
699 overview of RSL change at the three data sites over the last two millennia. Panel B focuses on
700 the period covered by the new proxy RSL data (last 800 years). Key: ^{14}C-dated isolation basin-
701 derived RSL data (black triangles, Aasiaat: Long et al. (2003), Sisimiut: Long et al. (2009),
702 Nanortalik: Sparrenbom et al. (2006a), Bennike et al. (2002)); ^{14}C-dated salt marsh-derived RSL
703 data (white squares, Long et al., 2011, this issue).

704

705

706

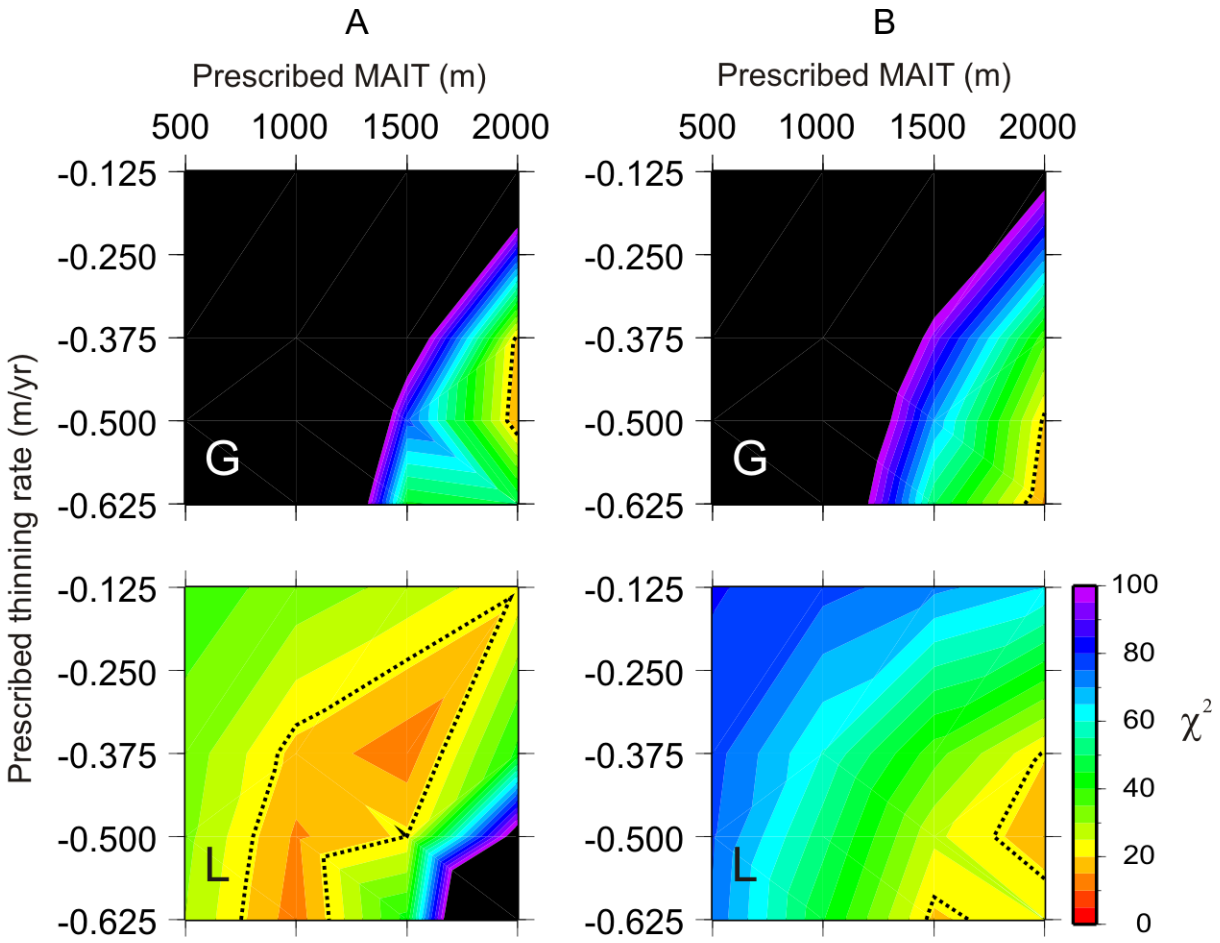

Figure 3 Chi squared plots displaying the degree of misfit for combinations of ice thinning rates (y axis) and chosen MAIT values (x axis). The chosen period of thinning is timed to coincide with the observed slowdown in RSL at (400 yrs BP to present, Panel A) and the Medieval Climatic Anomaly (1200-800yrs BP, Panel B). The chi-squared plots labelled 'G' (growth) and 'L' (loss) refer to the adopted rate of ice thickness change above the prescribed MAIT: +0.12 and -0.07m/yr, respectively. Dotted lines in the chi-squared plots denote the combinations of thinning rate and thinning area which produce RSL trends with a statistically equivalent fit (95% confidence interval).

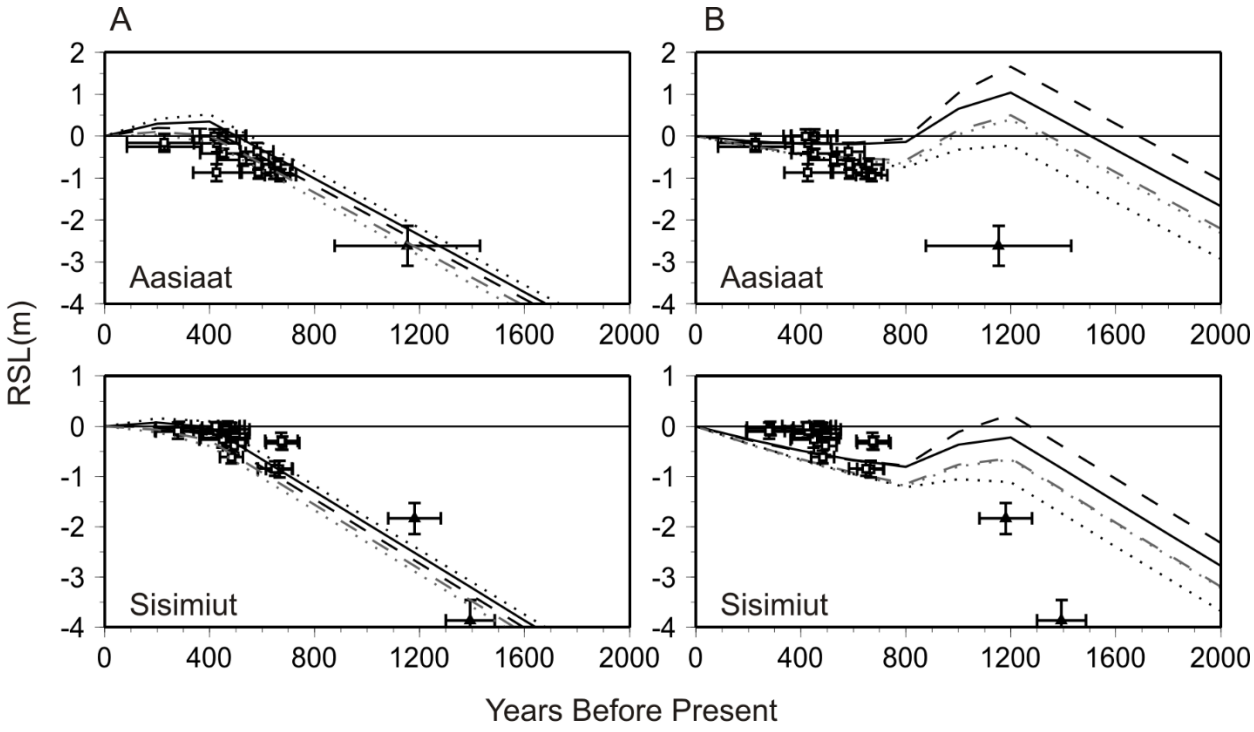

Fig. 4: RSL curves at each site calculated using optimal model parameters (see Table 1 for key). Panel A shows results for thinning during the period from 400 years BP to present and Panel B shows results for thinning during the period 1200-800 years BP.

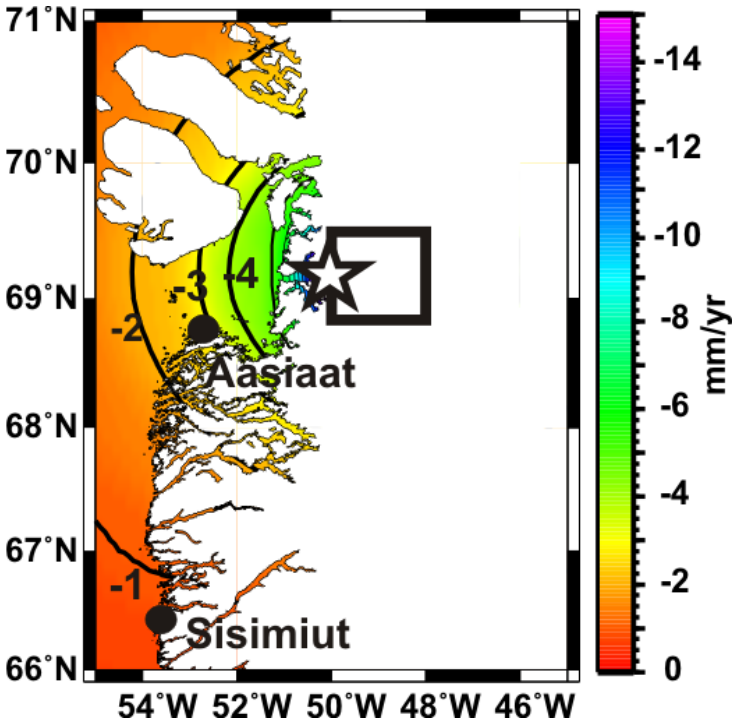

Figure 5: RSL fingerprint illustrating the local sea-level change generated by thinning of Jakobshavn Isbrae. The predicted sea-level change represents the immediate (elastic) land deformation and gravitational response to ice loss of 4m/yr over the region outlined, corresponding to an ice volume loss of 26 km^3/yr. The grounding line of Jakobshavn Isbrae is marked with a star. Note that the sea-level fingerprint may be linearly scaled for differing rates of ice loss or growth.

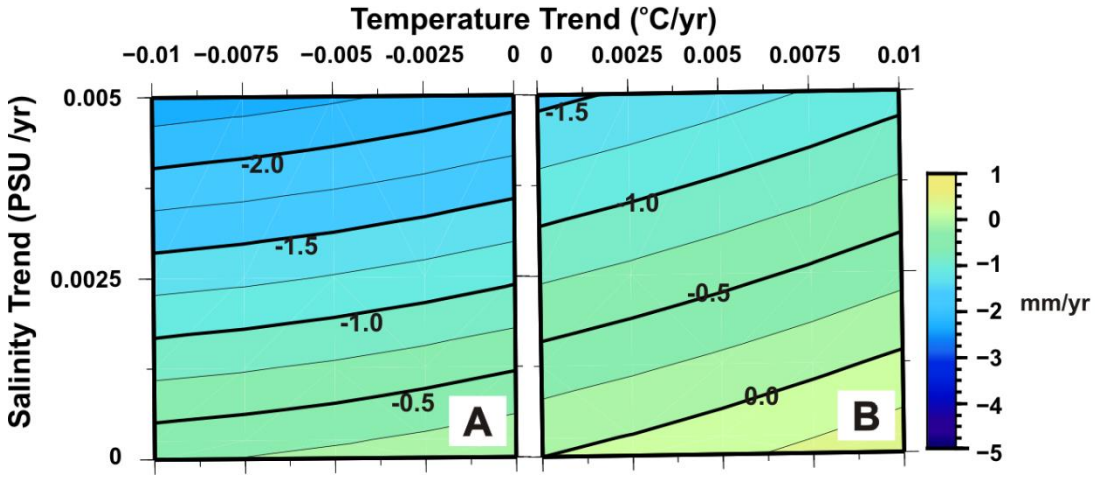

743

744 Figure 6: Predicted trends in steric height for cooling and salinification (Panel A) and warming and
745 salinification (Panel B) of the upper 500m of the water column. These perturbations are applied
746 to represent plausible changes to the water during a LIA climate. Panel A represents trends in
747 steric height as a result of cold conditions during the LIA. Panel B represents an alternative
748 scenario of ocean warming due to reduced meltwater flux (e.g. as in Krawczyk et al. (2010))

749

750

751

752

753

754

755

756

757 **Tables**

Key for RSL plots in Fig. 4	X^2	MAIT (m)	Prescribed ice thickness change below MAIT	Prescribed ice thickness change above MAIT	Area Below prescribed MAIT	Eustatic Equivalent SL change over time period	400 year RSL rate predicted at Nanortalik
		(m)	(m/yr)	(m/yr)	(km^2)	(mm/yr)	(mm/yr)
Panel A: Peripheral Mass Loss 400 years BP to present							
Black solid line	11.7	1500	-0.375	-0.07	325540	0.5	-1.53
Black dashed line	12.0	1000	-0.625	-0.07	134134	0.44	-1.19
Grey dashed line	14.1	1000	-0.5	-0.07	134134	0.4	-1.11
Black dotted line	14.8	2000	-0.5	0.12	643108	0.45	-1.66
Grey dotted line	18.2	2000	-0.375	0.12	643108	0.27	-1.04
Panel B: Peripheral Mass Loss 1200-800 years BP							
Black solid line	14.3	2000	-0.625	0.12	643108	0.63	-2.27
Black dashed line	16.5	2000	-0.5	-0.07	643108	0.9	-2.94
Grey dashed line	19.0	1500	-0.625	-0.07	325540	0.76	-2.11
Black dotted line	19.3	2000	-0.5	0.12	643108	0.45	-1.66
Grey dotted line	20.4	2000	-0.375	-0.07	643108	0.72	-2.32

758

759 Table 1: Details of the best fit model combinations obtained from the chi-squared analysis in Fig.

760 3

761

762

763

764

765

766

767

768

769

770 **Supplementary Data Information**

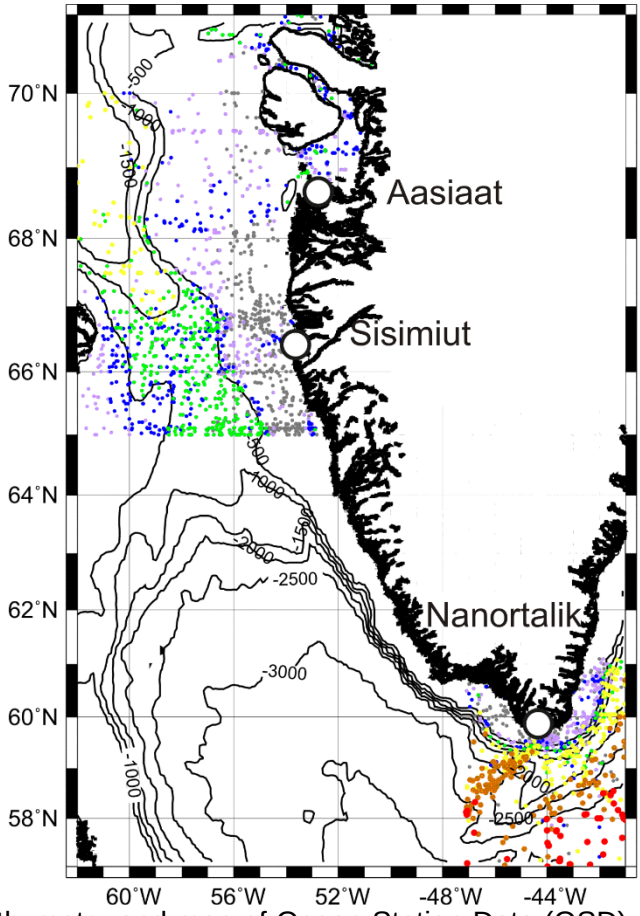

Figure S1: Bathymetry and map of Ocean Station Data (OSD) data used to calculate dynamic sea surface height and reference temperature and salinity profiles in Davis Strait and offshore Nanortalik. OSD data extending to 50m are coloured grey, to 150m (lilac), to 300m (blue), to 500m (green) to 1000m (yellow), to 2000m (orange) and to 3000m (red). Bathymetry is contoured every 500m. Stars indicate location of salt marsh data sites.

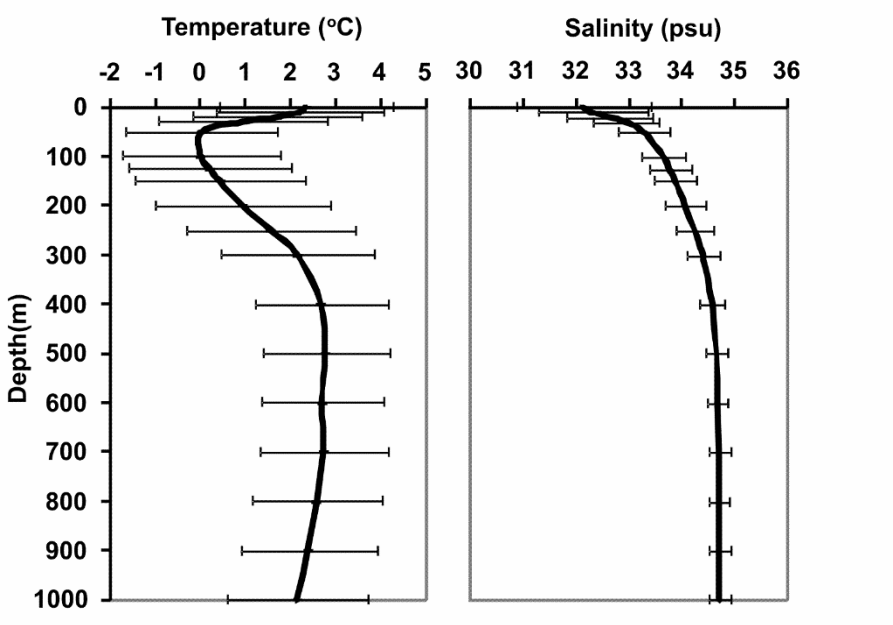

Figure S2: Average temperature and salinity profiles for the upper 1000m of ocean water in Davis Strait. Error bars indicate the standard deviation of measurements at the 2-sigma level due to both temporal and spatial variability.

792

Trend in steric height					Number of paired temperature and salinity profile by season with continuous measurements over specified depth interval used to calculate steric trends					
Time period	**Area**	**Depth Interval (m)**	**Trend (mm/yr)**	**2σ uncertainty (mm/yr)**	**Spring**	**Summer**	**Autumn**	**Winter**	**Total**	**% of profiles collected during Spring and Summer**
1928-1990	Davis Strait	0-50	0.19	0.06	155	1259	892	42	2348	92
1935-1997	Nanortalik	0-50	-0.68	0.16	177	524	178	26	905	77
1928-1990	Davis Strait	0-150	0.63	0.13	72	776	597	24	1469	93
1935-1997	Nanortalik	0-150	-0.45	0.28	126	423	106	18	673	82
1928-1990	Davis Strait	0-300	0.99	0.21	51	497	453	14	1015	94
1935-1997	Nanortalik	0-300	-0.42	0.29	111	284	71	15	480	82
1928-1990	Davis Strait	0-500	1.4	0.37	22	207	261	9	499	94
1935-1997	Nanortalik	0-500	0.03	0.32	107	159	54	17	337	79
1928-1990	Davis Strait	0-1000	2.1	0.7	0	19	33	0	52	100
1935-1997	Nanortalik	0-1000	-0.33	0.40	99	182	45	7	333	85
1935-1998	Nanortalik	0-2000	-0.57	0.44	50	92	27	5	174	82
1935-1997	Nanortalik	0-3000	-1.3	1.1	15	16	4	0	33	91

793

794 Table S1: Temporal distribution of OSD temperature and salinity data used in the calculation of
795 the reference temperature and salinity profiles (Fig. S2) and associated steric height trends. The
796 values in column 4 indicate the trends calculated for the specific depth interval noted in column
797 3.

798

799

800